Journal of Asian Earth Sciences 65 (2013) 3–12

Contents lists available at SciVerse ScienceDirect

Journal of Asian Earth Sciences

journal homepage: www.elsevier.com/locate/jseaes

Methane flux from miniseepage in mud volcanoes of SW Taiwan: Comparison with the data from Italy, Romania, and Azerbaijan

Wei-Li Hong [a,*], Giuseppe Etiope [b,c], Tsanyao Frank Yang [a], Ping-Yu Chang [d]

[a] Department of Geosciences, National Taiwan University, No. 1, Sec. 4, Roosevelt Road, Taipei 10699, Taiwan
[b] Istituto Nazionale di Geofisica e Vulcanologia, Sezione Roma 2, Italy
[c] Faculty of Environmental Science and Engineering, Babes-Bolyai University Cluj-Napoca, Romania
[d] Institute of Applied Geosciences, National Taiwan Ocean University, No. 2, Pei-Ning Road, Keelung City 202, Taiwan

ARTICLE INFO

Article history:
Available online 29 March 2012

Keywords:
Mud volcano
Miniseepage
Macro-seepage
Global methane emission

ABSTRACT

Mud volcanoes (MVs) are considered important methane (CH_4) sources for the atmosphere; gas is not only released from macro-seepage, i.e., from craters and visible gas bubbling manifestations, but also from invisible and pervasive exhalation from the ground, named miniseepage. CH_4 flux related to miniseepage was measured only in a few MVs, in Azerbaijan, Italy, Japan, Romania and Taiwan. This study examines in detail the flux data acquired in 5 MVs and 1 "dry" seep in SW Taiwan, and further compares with other 23 MVs in Italy, Romania and Azerbaijan. Miniseepage from the six manifestations in SW Taiwan MVs and seeps annually contribute at least 110 tons of methane directly to the atmosphere, and represents about ~80% of total degassing during a quiescent period. Combining miniseepage flux and geo-electrical data from the Wu-shan-ding MV revealed a possible link between gas flux and electrical resistivity of the vadose zone. This suggests that unsaturated subsoil is a preferential zone for shallow gas accumulation and seepage to the atmosphere. Besides, miniseepage flux in Chu-huo everlasting fire decreases by increasing the distance from the main gas channeling zone and molecular fractionation (methane/ethane ratio) is higher for lower flux seepage, consistently with what observed in other MVs worldwide. Measurements from Azerbaijan, Italy, Romania, and Taiwan converge to indicate that miniseepage is directly proportional to the vent output and it is a significant component of the total methane budget of a MV. A miniseepage vs. macro-seepage flux equation has been statistically assessed and it can be used to estimate theoretically at least the order of magnitude of the flux of miniseepage for MVs of which only the flux from vents was evaluated, or will be evaluated in future. This will allow a more complete and objective quantification of gas emission in MVs, thus also refining the estimate of the global methane emission from geological sources.

1. Introduction

Mud volcanoes (MVs) are the largest surface expression of hydrocarbon (methane-rich) fluids that migrate through neotectonic faults/fractures in petroleum bearing sedimentary basins. Their distribution, geology, formation mechanisms and impact to atmospheric methane budget are described in a wide literature (e.g., Milkov, 2000; Dimitrov, 2002; Etiope and Milkov, 2004; Etiope et al., 2011). Until few years ago, methane emission from MVs was generally attributed only to macro-seeps, i.e., visible gas manifestations like bubbling pools, salses and gryphons, and to eruptive events. Flux data were acquired in a few MVs (mainly in Azerbaijan) and most of them were rough estimates, often based on visual observations (Guliyev and Feizullayev, 1997; Dimitrov, 2002). Since 2002, the application to the MVs of the closed-chamber method, a system widely used to measure gas fluxes from soil respiration, wetlands or rice fields (e.g. Etiope et al., 2002), revealed that gas also exhales pervasively from the muddy ground around the visible vents, up to hundreds of meters from the MV center (Etiope et al., 2002, 2004a,b, 2011; Spulber et al., 2010). Thus, eruptions, fires and bubbles are not the only degassing processes. They are just the visible and localized component of a wider "breath" of the MV occurring potentially throughout its surface. The invisible exhalation is named "miniseepage" or "microseepage" depending on its intensity and distance from the macro-seeps. Initially only the term "microseepage" was generically used (Etiope et al., 2002, 2004a,b) but more recent surveys suggested the introduction of the term "miniseepage" to distinguish the high gas fluxes (typically hundreds to thousands of mg m^{-2} day^{-1}) from

* Corresponding author. Present address: College of Oceanic and Atmospheric Science, Oregon State University, 104 COAS Administration Building, Corvallis, OR 97331, USA. Tel.: +1 541 737 2467.

E-mail addresses: willyhong71@gmail.com (W.-L. Hong), etiope@ingv.it (G. Etiope), tyyang@ntu.edu.tw (T.F. Yang), pingyuc@mail.ntou.edu.tw (P.-Y. Chang).

1367-9120/$ - see front matter © 2012 Elsevier Ltd. All rights reserved.
http://dx.doi.org/10.1016/j.jseaes.2012.02.005

the lower "microseepage" fluxes (typically only up to hundreds of mg m^{-2} day^{-1}); the former usually distribute around the macro-seepage zone while the latter are distant from the vents, typically outside the muddy cover, and often independent of MV occurrence (Spulber et al., 2010; Etiope et al., 2011).

The invisible ground degassing was measured for the first time in 2001 in southern Italy and eastern Romania (Etiope et al., 2002, 2004a), then in four MVs in Azerbaijan (Etiope et al., 2004b), and more recently in Japan (Etiope et al., 2011) and Taiwan (this study). All the results clearly showed that methane fluxes are pervasive throughout most of the MV area and the amount of gas released into the atmosphere, calculated for the whole MV area, is comparable to, or even larger than the output from the macro-seeps alone. In other words, there is no a sharp jump of high flux from a vent to "zero emission" in the surrounding ground, but a gradual passage, leading to nil or "normal" negative methane fluxes only outside the MV area. Thanks to these studies, it was possible to elaborately improve estimates of global emission of methane from MVs to the atmosphere which likely exceed 10 Mt $year^{-1}$ (Etiope et al., 2011).

Miniseepage data from five MVs and one seep in SW Taiwan are presented and then integrated in a wider database including similar data from Italy, Romania and Azerbaijan. We include discussions of gas fluxes around a "dry" (no-water) gas seep with everlasting fire in SW Taiwan, which is not a MV but it provides further elements to understand the distribution of invisible gas seepage around a macro-seep. For the 5 MVs, their main features including flux magnitude, distribution and spatial variability are examined. Furthermore, gas flux data of a MV in Taiwan are compared with measurements of electrical resistivity in the vadose zone in order to evaluate the miniseepage distribution in relation to the fluid saturated and unsaturated subsoil conditions. A miniseepage vs. macro-seep flux equation is then statistically assessed: such an equation can be used to estimate theoretically the flux of miniseepage for MVs of which only the flux from vents is known, allowing a more complete and objective quantification of gas emission from MVs.

In this study, all the gas "flux" results will be presented in three forms with corresponding units which are flux (mg m^{-2} day^{-1}), output (ton $year^{-1}$), and emission factor (ton km^{-2} $year^{-1}$). Flux is the fundamental way we expressed our miniseepage flux results. Miniseepage output can be derived by different upscaling techniques (e.g., Etiope et al., 2011). Macro-seepage results are reported as output. Emission factor is then defined as summation of mini- and macro-seepage output divided by the area of each MV (Etiope et al., 2011).

2. Measurement methods for miniseepage

Miniseepage measurements were made, everywhere, by using the closed-chamber method, a technique initially developed for studies on the exchange of carbon and nitrogen bearing gases at the soil-atmosphere interface, such as soil respiration (e.g., Livingston and Hutchinson, 1995; Norman et al., 1997). The technique was then applied to detect positive flux of methane migrating from deep hydrocarbon reservoirs (Klusman et al., 2000), from coal mines (Thielemann et al., 2000) and gas exhalations in geothermal or volcanic areas (e.g., Hernandez et al., 1998; Cardellini et al., 2003; Etiope et al., 2005; Lan et al., 2007).

To date, closed-chamber seepage measurements in MVs have been carried out only in Italy, Romania, Azerbaijan and Japan by Istituto Nazionale di Geofisica e Vulcanologia (e.g., Etiope et al., 2004a,b, 2007, 2011), in Romania by Babes-Bolyai University of Cluj-Napoca (Spulber et al., 2010) and in Taiwan by the National Taiwan University (NTU; this study). All chambers used in Europe and Asia were similar to the "Crill" system (Norman et al., 1997): the shape is always circular, with volumes from 5 to 15 l (height 4–10 cm) and the material is PVC, stainless-steel or aluminum (Fig. 1). An internal fan is generally used to assure mixing of gas and air inside the chamber.

In the methodology used by INGV for Azerbaijan, Italy (Sicily) and Romania MVs (Table 1; Etiope et al., 2002, 2004a,b) gas samples were collected twice or three times into syringes at time intervals varying from 1 to 20 min after the deployment of the chamber (Fig. 1a), and methane was analyzed in duplicate by portable gas chromatograph with flame ionization detector. Gas flux was calculated on the basis of the concentration increment with time, chamber height, temperature and pressure (e.g., Livingston and Hutchinson, 1995). The methane flux F is generally expressed in terms of mg m^{-2} day^{-1} and it is given by the equation:

$$F = (V_c/A_c)x(c_2 - c_1)/(t_2 - t_1) \quad (1)$$

where V_c (m^3) is the volume of the chamber, A_c (m^2) its area, c_1 and c_2 (mg m^{-3}) are methane concentrations at times t_1 and t_2 (days). The flux measurement reproducibility was within 13% and 20% for fluxes below and above 5000 mg m^{-2} day^{-1}, respectively. Measurements of MVs in north-central Italy (Table 1; Etiope et al., 2007) were performed by directly connecting the chamber on line with a portable solid state CH_4 detector (METREX 2, Huberg; detection limit 1 ppmv, accuracy 10%, leading to a flux detection limit of 30 mg m^{-2} day^{-1} with 10–20 min of accumulation time, depending on chamber size). The latest data in Transylvania (Spulber et al., 2010) and Japan (Etiope et al., 2011, not included in this work) were acquired by using a new closed-chamber system (Fig. 1b) developed by West Systems srl (Italy) in collaboration with INGV; the system is equipped with portable CH_4 and CO_2 sensors and wireless data communication to a palm-top computer; the gas fluxes are calculated through a linear regression of the gas concentration build-up in the chamber. The CH_4 sensor includes semiconductor (range 0–2000 ppmv; lower detection limit: 1 ppmv; resolution: 1 ppmv), catalytic (range: 2000 ppmv – 3% v/v), and thermal conductivity (3–100% v/v) detectors (precision of 5%). Maximum accumulation time of 15 min allowed detecting fluxes down to 10 mg m^{-2} day^{-1}. The CO_2 detector is a double beam infrared sensor (LiCor) with accuracy of 2%, repeatability ±5 ppmv and full scale range of 2000 ppmv. The chamber is then equipped with a Nafion® dryer for humidity removal. Laboratory tests based on known gas fluxes suggested a reproducibility better than 5% (Etiope et al., 2011).

Gas flux measurements in Taiwan were based on discrete gas sampling (up to five repeated samplings at one location with 1–5 min time interval) from a fan-equipped aluminum chamber. Gas samples were then stored in 10 ml serum vials which were capped with septa and filled with saturated sodium chloride solution before sampling (Fig. 1c and d). The saturated sodium chloride can effectively decrease the solubility of methane in water at room temperature as Cramer (1984) demonstrated in his experiments. The concentration of CH_4, CO_2 and ethane (C_2H_6) is then measured in laboratory by GC (gas chromatograph; SRI 8610C) with flame ionization detector. Detection limit for CH_4, CO_2, and C_2H_6 are 0.0011, 38.7, and 6.3 ppmv (Lee et al., 2005), respectively; the analytical error for the three gases is within 2% (Lee et al., 2005). Gas flux is determined by Eq. (1). Detection limit is ca. 10 mg m^{-2} day^{-1}. This methane flux detection limit is similar to the limit that can be measured by West Systems chambers even though GC is capable of measuring lower concentration comparing to the semiconductor detectors utilized by West Systems. The similar flux detection limit is due to the similar length of chamber-deploy time between the two systems. The measurements at each MV were distributed as evenly as possible to obtain unbiased flux estimation.

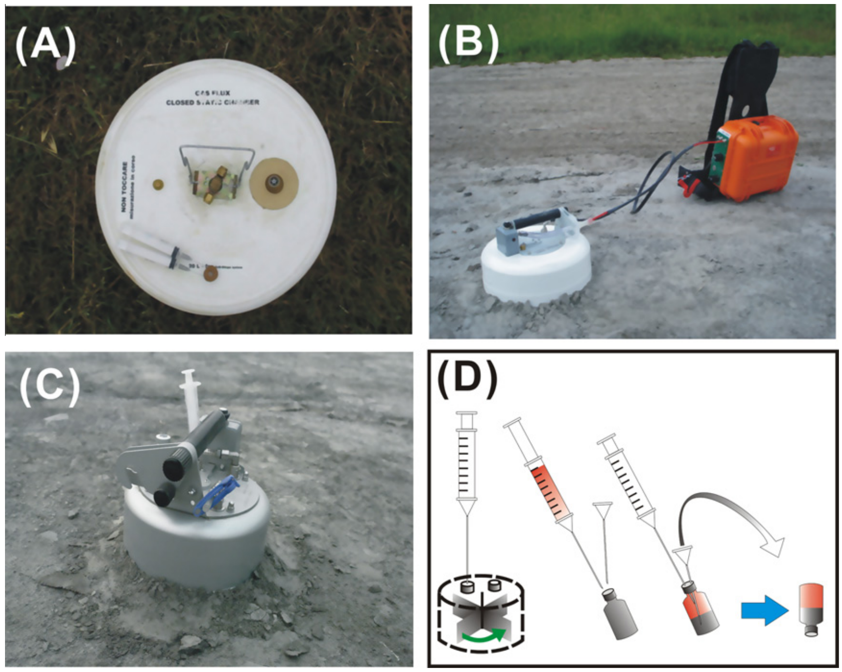

Fig. 1. Closed-chamber systems used in miniseepage measurements. (A and B) chambers used by INGV; (B) is a West Systems instrumentation, with the chamber connected to a semiconductor sensor. (C) Chamber used by NTU and sample storage procedure (D).

3. Miniseepage flux magnitude and distribution in SW Taiwan MVs

3.1. General description of the MVs in SW Taiwan

Methane flux in Taiwan was measured in five MVs named Shi-ao-kung-shuei (SKS), Gung-shuei-ping (GSP), Shin-yang-nyu-hu (SYNH), Wu-shan-ding (WSD) and Li-yu-shan (LYS), and, for comparison, in a "dry" seep independent of mud volcanism, characterized by an everlasting fire named Chu-huo (CH) (Fig. 2). The distribution of these MVs and seep is closely associated with active tectonic regimes in SW Taiwan as described in Yang et al. (2004). SKS locates closely to the axis of Gu-ting-keng structural anticline; GSP and LYS are at the Coastal Plain; SYNH and WSD are close to the active Chi-shan Fault; CH locate at the southern end of Taiwan island which is now actively uplifted (Huang et al., 1997). Geologic setting of these active areas are described by Mouthereau et al. (2001) and Huang et al. (2006).

The tectonic structures of such active areas, as well as MVs, extend seaward to the northern continental slope of South China Sea (Lin et al., 2008). Many mud diapirs and offshore MVs had been identified by Chiu et al. (2006) from seismic and chirp sonar surveys as shown in Fig. 2. Besides, both high methane flux in the sediments and high methane concentration in water column had been observed previously (Yang et al., 2006; Lin et al., 2006; Chuang et al., 2006, 2010). Due to the similarity in geological background and between the distributions of MVs onshore and offshore SW Taiwan, our survey could potentially provide an analog to offshore MVs.

Except for the LYS, the degassing behavior of the other four MVs is more or less constant and it is characterized by continuous bubbling from multiple craters. Multiple craters with constant bubbling on the top of craters are typically observed indicating continuous gas emission from the macro-seeps (Yang et al., 2004; Chao et al., 2010). Craters are usually surrounded by un-vegetated dry mud where most of our measurements were performed. Vegetation usually appears several tens of meters away from the craters where there is no muddy cover and gas leakage is much lower. Some craters may change locations from time to time inferring lateral migration of the seepage channels. Different from these four MVs, the degassing behavior of LYS is more frequently characterized by explosive eruptions (2–3 times per year with eruptions lasting 6–12 h). Several vigorous explosions at LYS had been witnessed and recorded by local inhabitants. Mud expelled from the explosions could be up to ~5 m. Flames lit by local habitants can be up to ~10 m high. Besides those MVs, CH, the dry seep, is characterized by continuous degassing which is however visible thanks to a flame lit by local habitants.

3.2. Miniseepage fluxes and total emission

The following flux estimation was based on 187 measurements conducted in a relatively calm degassing period in 2006 (no significant blow-ups or eruption were observed during our survey) at the six studied locations. The number of measurements at each location may vary depending on the area of measureable dry soil. The largest two MVs, GSP and WSD, hosted 43 and 93 measurements, respectively. In the smaller MVs (SYNH, SKS, and LYS) and "dry" seep (CH), 6, 8, 12 and 25 measurements were made. Significant CH_4 and CO_2 fluxes were measured in all six locations (Fig. 3). Besides, considerable C_2H_6 fluxes (up to 8.3×10^5 mg m^{-2} day^{-1}) were only detected at CH. This is consistent with the C_2H_6 concentration which is higher in the CH gas vent and much lower in the other MVs, as reported by Yang et al. (2004). The ratios between miniseepage CH_4 and C_2H_6 fluxes at CH is usually less than 100 which is consistent with their corresponding concentration ratios. At certain points where C_2H_6 fluxes are considerably high, the flux ratio could even be less than 10 (Fig. 4). Such ratios imply the thermogenic origin of the gas at CH.

Average miniseepage CH_4 flux in all locations ranges from 10^0 to 10^5 mg m^{-2} day^{-1}, with the highest flux at CH and the lowest flux at SKS. Average miniseepage CO_2 flux ranges from 10^0 to 10^3 mg m^{-2} day^{-1}; the highest and lowest fluxes were observed at CH and WSD respectively. In order to estimate the annual con-

Table 1
Miniseepage and macro-seepage flux data from 28 mud volcanoes and one everlasting fire.

Country	Mud volcano	Measured area (km^2)	MV size[a]	Miniseepage output (ton $year^{-1}$)	Macro-seep output (ton $year^{-1}$)	Total emission (ton $year^{-1}$)	Emission factor (ton km^{-2} $year^{-1}$)	References
Azerbaijan	Lokbatan	0.1	Large	19.2	n.m.	19.2	192	Etiope et al. (2004a)
	Dashgil	0.6	Large	104	623	727	1211	Etiope et al. (2004a)
	Kechaldag	0.05	Large	5.8	4	9.8	196	Etiope et al. (2004a)
	Bakhar	0.05	Large	5.5	8.4	14	230	Etiope et al. (2004a)
Italy	*Sicily*							
	Maccalube	1.4	Large	374	20	394	281	Etiope et al. (2002)
	Occhio abisso	0.001	Small	0.49	2.2	2.7	2700	Etiope et al. (2002)
	North-central Italy							
	Frisa	0.005	Small	1.9	n.m.	1.9	380	Etiope et al. (2007)
	Ospitaletto	0.001	Small	0.6	0.8	1.4	1400	Etiope et al. (2007)
	Pineto	0.0002	Small	0.6	0.1	0.7	3500	Etiope et al. (2007)
	Rivalta	0.003	Small	10.8	1.2	12	4000	Etiope et al. (2007)
	Regnano	0.006	Medium	29	5	34	5667	Etiope et al. (2007)
	Nirano	0.08	Large	26.4	6	32.4	405	Etiope et al. (2007)
	Dragone	0.002	Small	0.15	0.2	0.35	175	Etiope et al. (2007)
	Serra de Conti	0.015	Medium	3	0.3	3.3	220	Etiope et al. (2007)
Romania	Paclele Mici	0.62	Large	128	255	383	618	Etiope et al. (2004b)
	Paclele Mari	1.62	Large	430	300	730	451	Etiope et al. (2004b)
	Fierbatori	0.025	Medium	20	17	37	1480	Etiope et al. (2004b)
	Trasylvania							
	Homorod	0.005	Small	0.5	0.5	1	200	Spulber et al. (2010)
	Monor	0.002	Small	13.9	2.1	16	8000	Spulber et al. (2010)
	Filias	0.00005	Small	0.1	0.38	0.49	9800	Spulber et al. (2010)
	Porumbeni Mici	0.00004	Small	0.27	0.2	0.47	11750	Spulber et al. (2010)
	Cobatesti	0.00008	Small	0.2	1.4	1.6	20,000	Spulber et al. (2010)
	Boz	0.00002	Small	0.01	0.19	0.20	10,000	Spulber et al. (2010)
Taiwan	Shing-yang-nyu-hu	0.0004	Small	0.5	1.7	2.2	5500	This study
	Gung-shuei-ping	0.005	Small	0.004	1.1	1.1	220	This study
	Shiao-kung-shuei	0.0003	Small	8.8E-5	1	1	3333	This study
	Li-yu-shan	0.0003	Small	0.0006	n.m.	0.0006	2	This study
	Wu-shan-ding	0.006	Medium	30.2	4.8	35	5833	This study
	Chu-ho	0.0007	Fire	75.5	–	75.7	107,860	

nm = Not measurable two to three times explosive emission every year.
[a] Size is distinguished on the basis of the diameter of the muddy cover for single-dome MV or of the area of the multiple vents as follows: Large: diameter > 100 m; medium: 20 < diameter < 100 m; small: <10 m.

tribution of CH_4 and CO_2 through miniseepage to the atmosphere, we calculated the total annual output at these six locations as follow:

$$\overline{E}_{miniseep}(\text{ton year}^{-1}) = \overline{F}_{miniseep}\left(\text{mg m}^{-2}\text{ day}^{-1}\right) \times A\ (\text{m}^2) \times 365(\text{day year}^{-1}) \times 10^{-9}(\text{ton mg}^{-1}) \quad (2)$$

where $\overline{F}_{miniseep}$ is the average of all CH_4 or CO_2 flux measurements at each location (being the surveyed area, A, quite small) and $\overline{E}_{miniseep}$ is the average of miniseepage output. The total annual miniseepage outputs of CH_4 and CO_2 from all six locations are then ~110 tons and ~6.3 tons, respectively.

Methane output data from macro-seeps are available for two different periods, the first during a relatively low degassing activity (as in our miniseepage survey), with an output of 28 tons $year^{-1}$ (Yang et al., 2004), and the second which was characterized by higher degassing activity (980–2010 tons $year^{-1}$; Chao et al. (2010). Total CH_4 emission (miniseepage + macro-seepage) for low degassing activity would be then around 130 tons $year^{-1}$. It is very likely that in the period with the higher macro-seep fluxes as measured by Chao et al. (2010) miniseepage was also higher. In particular, the YNH mud volcano was extinct during our miniseepage survey, but its CH_4 output measured by Chao et al. (2010) was 3–4 orders of magnitude higher than that reported by Yang et al. (2004). This suggests that miniseepage may also vary significantly during the MV life; this should be verified by measurements repeated in different stages.

3.3. Miniseepage distribution around a dry seep

The fire zone emits more CH_4, CO_2, and C_2H_6 to the atmosphere (average flux for the three gases are 3×10^5 mg m^{-2} day^{-1} of CH_4, 1×10^4 mg m^{-2} day^{-1} of CO_2, and 3×10^3 mg m^{-2} day^{-1} of C_2H_6) compared with other MVs in SW Taiwan. The order of magnitude of the CH_4 flux is the same of that measured in other burning seeps in Europe (e.g., Etiope et al., 2007). The high flux of "dry" seeps reflects a seepage system which is quite different from that of MVs (Etiope et al., 2009), in terms of water content, gas flow velocity and permeability in the subsoil (as discussed in Section 4.1). At CH, soil and subsoil are mostly composed of sands and pebbles and are therefore quite dry and more permeable (Fig. 4A) compared to the ground of MVs. Miniseepage of C_2H_6 and CH_4 exhibits a significant spatial variation at this location (Fig. 4). High C_2H_6 and CH_4 fluxes were observed in the everlasting fire zone (13 flux measurements ranging from 3.4×10^4 to 1.9×10^6 mg m^{-2} day^{-1} for CH_4 and 1.7×10^3 to 8.3×10^5 mg m^{-2} day^{-1} for C_2H_6) while low or nil C_2H_6 flux (seven measurements from below the detection limit to 5×10^3 mg m^{-2} day^{-1}) and high CH_4 fluxes (from 2×10^2 to 5×10^5 mg m^{-2} day^{-1}) were detected at the ground without vegetation outside the everlasting fire zone. Both C_2H_6 and CH_4 fluxes (five measurements) were below detection limit ($<1 \times 10^1$ mg m^{-2} day^{-1}) at the ground with vegetation outside the everlasting fire zone.

Such a zonation in CH_4 and C_2H_6 miniseepage flux could be the result of differential molecular fractionation. As observed in other seeps and MVs, during migration to the surface the gas mixture

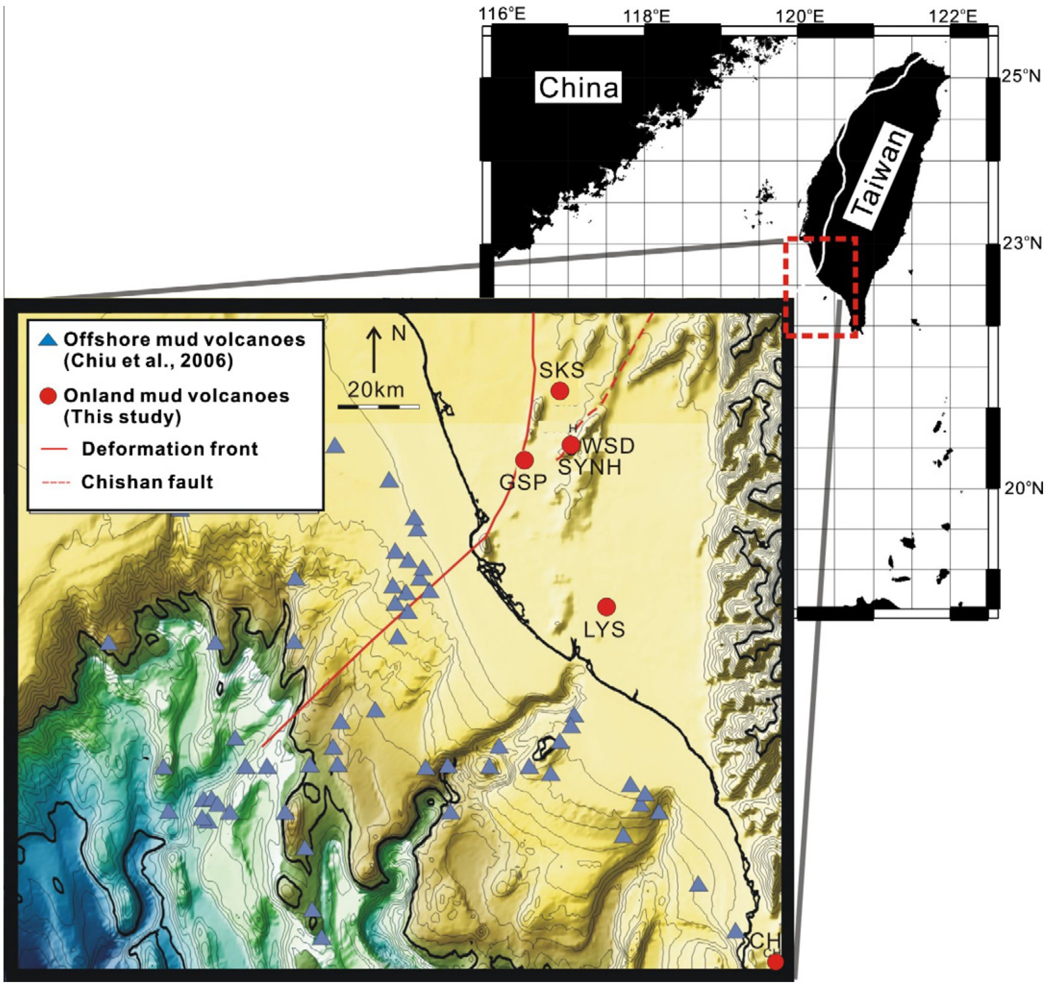

Fig. 2. Distributions of mud volcanoes and seeps studied in SW Taiwan. Offshore mud volcanoes are shown for comparison.

can be affected by molecular fractionation, that is a progressive separation of CH_4 from other heavier alkanes, due to differential solubility and molecular adsorption on solid grains, so that gas at the surface is dryer (more methane and less ethane and propane) than the deeper original gas (Etiope et al., 2009). This fractionation seems to be inversely proportional to the gas flow (Etiope et al., 2007, 2011; Chao et al., 2010). The center of CH everlasting fire zone is the main seepage channel where the velocity of gas is higher than surrounding area and the bulk gas mixture ascends rapidly without substantial fractionations. As the distance from the main seepage channel increases, subsoil permeability likely decreases which results in lower advective velocity of gas, higher gas–water–sediment interactions, and a more substantial molecular separation comparing to the center. As a consequence, C_2H_6 flux to the atmosphere decreases rapidly.

3.4. Miniseepage flux and vadose zone in Wu-shan-ding MV

The comparison between flux measurements in WSD and a geo-electrical survey (Chang et al., 2010) conducted in the same period suggests a possible link between miniseepage flux and subsoil condition. From the distribution of all flux measurements in Fig. 5A, high gas fluxes in WSD are clustered in two groups: one group at the northeast of the survey area, the other group extends from the southeast corner to the northwest corner of the survey area. The electrical resistivity, which is an indication of unsaturated vadose zone, increases in the high flux zone, as evidenced by three profiles (Fig. 5B). This would suggest that miniseepage flux increases as the water content in subsoil decrease. Also, completely saturated subsoil can reduce gas leakage to the surface.

4. Gas emission database from 28 MVs in Italy, Romania, Azerbaijan, and Taiwan

Table 1 summarizes the miniseepage and macro-seepage output data acquired in 28 European and Asian MVs plus one "dry" seep site (CH) for comparison. Total emission in Table 1 is the sum of mini- and macro-seepage outputs. Emission factor is thus the total emission divided by the measured area of individual MV which may be different from the actually area.

4.1. Gas flux vs. subsoil condition

Our experience suggests that in many cases diffuse exhalation of gas in a MV strongly depends on the water content of the ground. Wet conditions, such as those typically occurring along fresh mud flows from active gryphons, seem to produce an efficient impermeable cover to gas. However significant gas fluxes were also detected just in correspondence with fresh mud around vents (Etiope et al., 2011). The existence of wet mud on the surface, as a result of mud flow from craters or gryphons, does not necessarily imply saturated conditions below the ground. Vice versa, dry mud on the surface may hide a wet, saturated vadose zone. As

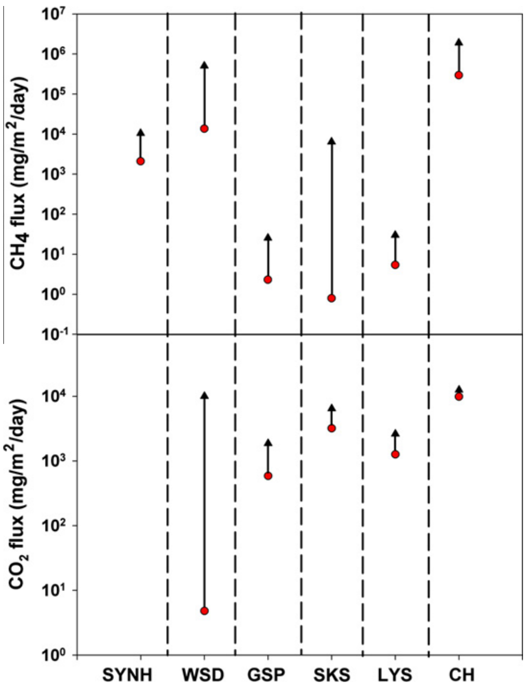

Fig. 3. Results of CH_4 and CO_2 miniseepage flux from mud volcanoes and seep in SW Taiwan. Arrow shows the upper range of flux with error at each mud volcano. Lower range of flux for all locations is below detection limit (SYNH: Shing-yang-nyu-hu; WSD: Wu-shan-ding; GSP: Gung-shuei-ping; SKS: Shiao-kung-shuei; LYS: Li-yu-shan; CH: Chu-ho).

we have demonstrated in the previous paragraph, the saturation of subsoil probably plays an important role in modulating surface miniseepage flux. Probably more factors including gas pressure gradient, subsoil permeability and water content determine the intensity of miniseepage at the surface.

Due to the possible impermeable barrier induced by water on the surface (fresh mud) or in the subsoil, the flux measurements are generally performed in the areas uncovered by wet mud. In this respect, two different configurations of MV are depicted in Fig. 6. Type A represents, typically, small or medium-size MVs that are almost completely covered by mud flows or wet mud (i.e., wet-mud area larger than dry area). In this condition, miniseepage measurements are possible (or have higher chance to detect gas migration signals) only at the external flanks or MV margin. MVs of this type include Paclele Mici, Beciu (in Romania), Frisa, Ospitaletto (Italy), Gung-shuei-ping, Shing-yang-nyu-hu, and Shiao-kun-shuei (Taiwan). An example is shown in Fig. 7A. For type B MV, the release of water, and consequent mud flow, is spatially relatively limited. Most of the ground is dry, even around bubbling pools (e.g., Pineto, Maccalube, Regnano, Nirano in Italy; Paclele Mari, Homorod and Fierbatori in Romania; Wu-shan-ding and in Taiwan; almost all MVs in Azerbaijan, given their size). So, type B allows a wider miniseepage survey. An example is shown in Fig. 7B.

In large type B mud volcanoes, two or three main different seepage zones can be recognized:

- *high degassing zone*: flux in the order of 10^3–10^5 mg m^{-2} day^{-1}; generally coincident with the ground around bubbling pools and dry vents, typically at the central part of the mud volcano.
- *"normal" degassing zone*: flux in the order of 10^1–10^3 mg m^{-2} day^{-1} (generally <5000). It is the largest part of the MV, including summit area (when dry), and flanks.
- *Low degassing zone*: flux <100 mg m^{-2} day^{-1}. It is generally at the MV margins and outside the MV boundary, but can occur also in central sectors, between the active zones. This exhalation should be more properly named "microseepage" (Spulber et al., 2010; Etiope et al., 2011)

This "zonation", however, does not appear in small mud volcanoes, especially those belonging to type A.

4.2. Total emission from miniseepage

The total gas output from miniseepage is estimated by identifying homogeneous sectors showing similar fluxes (i.e., with low variance): for each sector the output is given by multiplying the mean flux with the sector area; alternatively, the output from each "homogeneous" sector can be derived by kriging or natural neighbor interpolation methods (Spulber et al., 2010; Etiope et al., 2011). Total miniseepage emission is then the sum of the outputs from the several sectors. This is a standard "emission factor" based up-scaling method, also recommended by the EMEP/EEA Atmospheric Emission Inventory Guidebook (EMEP-EEA, 2009). The estimated methane outputs are summarized in the last columns of Table 1 and in Fig. 8. The Taiwanese data shown in Table 1 refer only to miniseepage measured over dry mud. From Fig. 8, it is intuitive that more CH_4 is emitted when the area of MV is larger. This relationship indicates that larger MVs are more important CH_4 emitter in terms of total quantity. However, as we are going to discuss in the next paragraph, if the amount of CH_4 emitted from a certain area during a certain time is calculated (i.e. emission factor), smaller MVs can actually emit more CH_4 to atmosphere on a unit area base (Fig. 9B).

4.3. Miniseepage vs. microseepage

Beyond the data-set of Table 1, a fair number of measurements were also performed outside the MV boundaries, which are generally identified with the end of the older mud cover and the margin

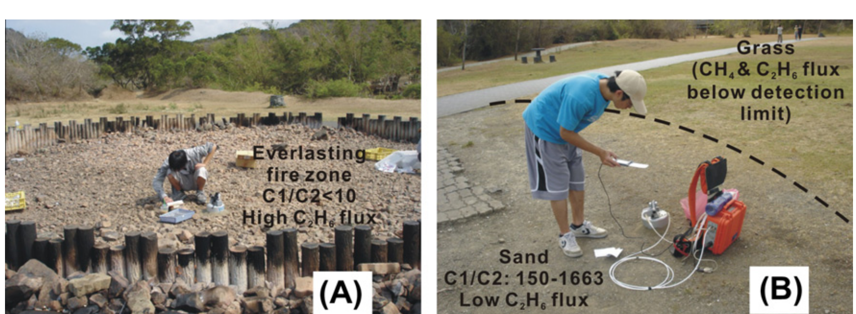

Fig. 4. Miniseepage measurements at the CH everlasting fire. (A) High CH_4 and C_2H_6 fluxes were observed inside the everlasting fire zone. (B) High CH_4 flux but low C_2H_6 flux were observed at the ground without vegetation outside the fire zone. CH_4 and C_2H_6 flux were both below detection limit several meters far from the central vent.

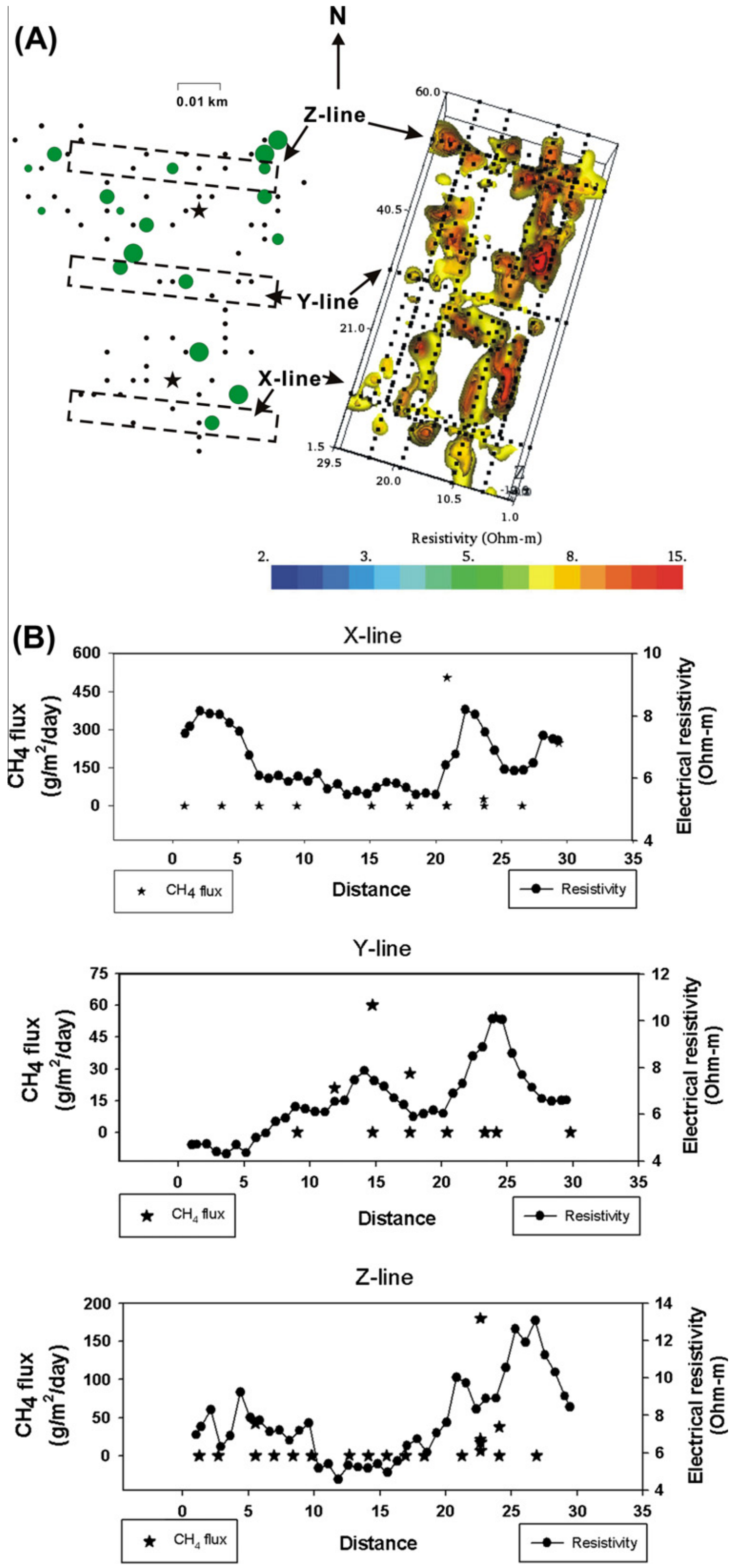

Fig. 5. Spatial distribution of miniseepage CH_4 flux in WSD and 2D electrical resistivity surveys conducted by Chang et al. (2010). (A) Distribution of methane flux is shown on the left. Green dots represent location with significant miniseepage flux while black dots are spots with flux below detection limit. Size of green dots is proportional to flux magnitude. Result of electrical resistivity from Chang et al. (2010) is shown on the right for comparison. Two zones of high miniseepage flux were observed (northeast of the survey area and a NW–SW elongation across the area) which seems to have some spatial correlation with the electrical resistivity. (B) Both flux and electrical resistivity results along the three E–W profiles (*X*, *Y*, and *Z*-lines) were plotted for detail comparison. Again, such spatial correlation is emphasized; such a correlation may suggest a link between miniseepage flux and subsoil water content. (For interpretation of the references to color in this figure legend, the reader is referred to the web version of this article.)

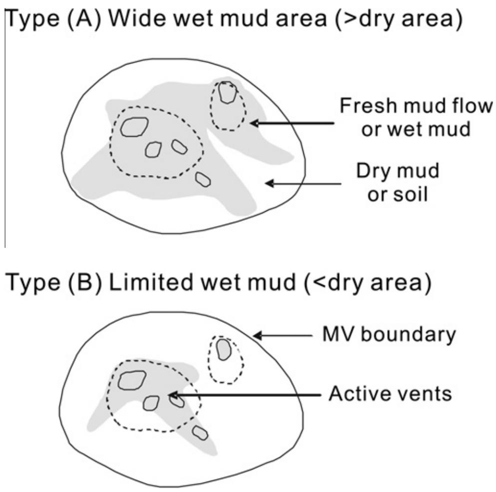

Fig. 6. Two main configurations of mud volcanoes in relation with mud flow extension and dry-mud or soil distribution. In type (A), miniseepage may not be detectable on the MV summit or around the main crater zone, but only along the external flanks. Type (B) allows a wider miniseepage survey.

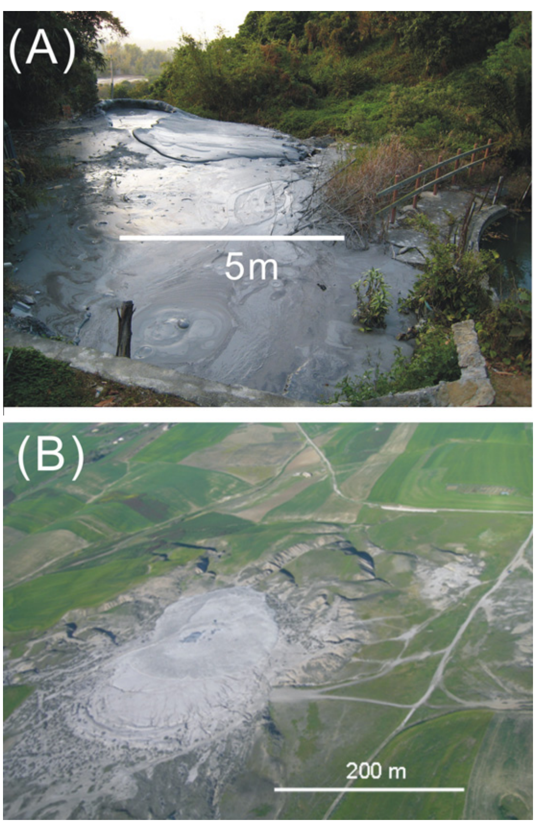

Fig. 7. Examples of mud volcanoes. (A) Shing-yang-nyu-hu (SYNH) MV in Taiwan, classified as type-A. (B) Aerial view of Maccalube MV, Italy, classified as type-B.

of the grassland and trees. Positive methane fluxes have been detected at tens and hundreds meters from the MV boundaries, indicating that microseepage (see definition in Etiope et al., 2011) can be attributed to the MV if the flux clearly tends to zero (or to normal negative values) as the distance from the active MV zone increases. In some cases, instead, low CH_4 fluxes exist around MV zones just because they belong to the widespread microseepage related to faults and deep reservoirs, independently from the existence of mud volcanism. This kind of microseepage, a very important methane source on a global scale, is discussed elsewhere (Etiope and Klusman, 2010).

In analogy with the procedures for estimations of greenhouse gas emission recommended by EMEP/EEA guidelines (EMEP-EEA, 2009), we consider the MV "emission factor" as the sum of mini- and macro- output (tons year^{-1}) divided by area (km^2). For a more convenient statistical elaboration, the four factors, mini-, macro-seepage, area, and emission factor are converted into log-transferred form. Two linear correlations, miniseepage vs. macro-seepage (Fig. 9A) and emission factor vs. area (Fig. 9B), can be observed from our 29 data (LYS and CH are excluded). The linear regression formulas are

$$\mathrm{Ln(miniseepage\ output)} = 0.98 \times \mathrm{Ln(macro\text{-}seepage\ output)} + 0.24 \quad (3)$$

and

$$\mathrm{Ln(emission\text{-}factor)} = -0.34 \times \mathrm{Ln(area)} + 5.39 \quad (4)$$

where "Ln" denotes natural logarithm.

For the relationship between miniseepage and macro-seepage output, LOK and FRI are not included in the calculation due to lack of macro-seepage measurements; SKS and GSP are treated as outliers and excluded from the calculation, since they became inactive during the period of our survey compared to several years ago (Yang et al., 2004).

For these two relationships, significant tests and prediction intervals have been calculated. *F* test is applied in order to check whether the correlations are statistically significant. *F* value is calculated from MS_{reg} (mean of square regression) over MS_{res} (mean of square residual). This value is an indication of the relative contribution between regression and residual (or error). The null hypothesis of this test is the relative contribution of regression equals to it from residual (so that *F* will equals to 1). From our ANOVA table (Analysis of variance; Table 2), the *F* values for the two relationships are 23.7 and 48.9. Both of them are significantly higher than the threshold values ($F_{0.01}(1,26) = 7.677$ and $F_{0.01}(1,22) = 7.945$ from appendix *F* in Howell (2002)) for $\alpha = 0.01$, which means that there is only 1% of possibility that we would incorrectly reject the null hypothesis when in fact it is true. Thus, we can conclude that the null hypothesis has to be rejected; or in other words, the contribution from the regression is significantly larger than from residual. The 95% prediction intervals are calculated following

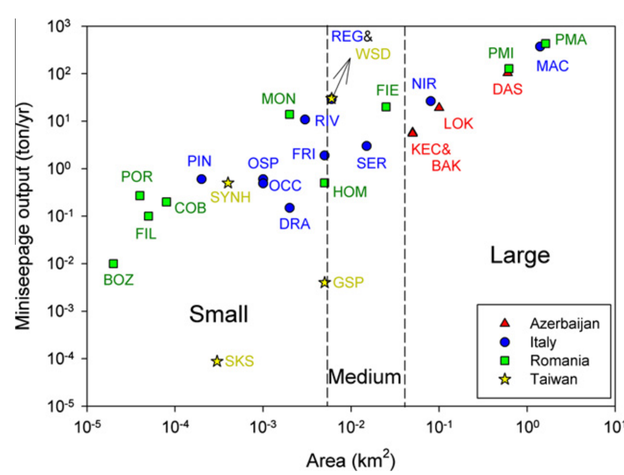

Fig. 8. Relationship between miniseepage output vs. mud volcano area. Larger MVs are more important CH_4 sources in terms of total quantity.

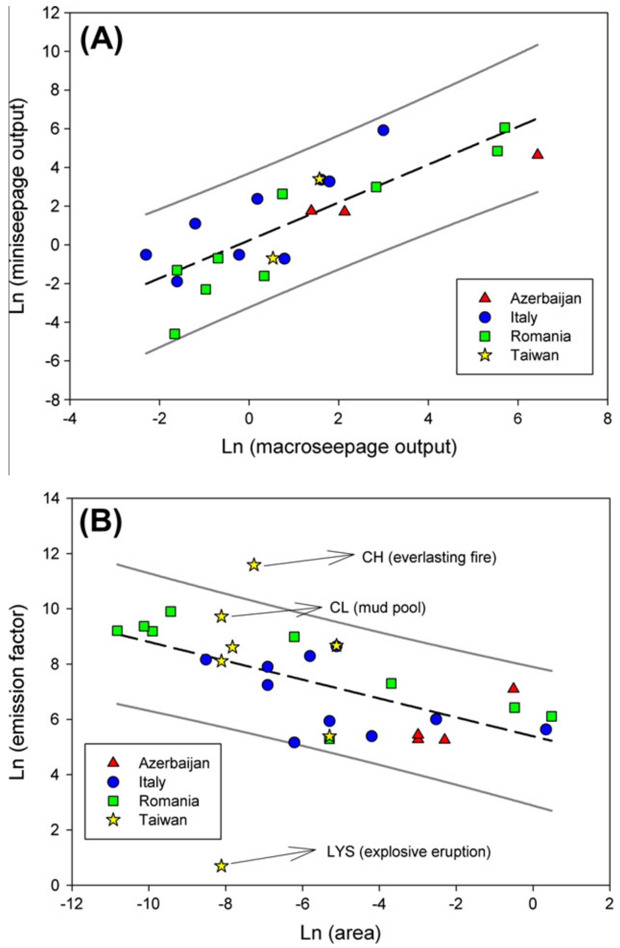

Fig. 9. Miniseepage vs. macro-seepage (A) and emission factor vs. area (B) correlations and regression formulas. Long dash lines are the regression lines; solid lines are 95% prediction intervals. (A) The positive correlation infers that, as macro-seepage, miniseepage also serves as the indication of MV activity. (B) Smaller MVs are actually more important CH_4 emitter on a unit area and unit time base.

Table 2
ANOVA table for (A) ln(area) vs. ln(emission-factor) and (B) ln(macro-seepage output) vs. ln(miniseepage output).

	df	SS	MS	*F*
(A)				
Total	22	178.60	8.12	
Regression	1	123.17	123.17	46.66
Residual	21	55.43	2.64	
Variables	coeff.	s.e.		
Slope	0.98	0.60		
Intercept	0.24	0.22		
(B)				
Total	26	65.02	2.50	
Regression	1	31.02	31.02	22.81
Residual	25	34.00	1.36	
Variables	coeff.	s.e.		
Slope	−0.34	0.51		
Intercept	5.39	0.08		

df: degree of freedom, SS: Sum of Squares, MS: Mean of Square, *F*: *F* statistic, s.e.: standard error of residuals.

Wilks (2006): predicted value ± 1.96 × $(MS_{res})^{1/2}$ which are shown as the dark gray lines in Fig. 9.

In general, higher macro-seepage output implies higher miniseepage output, regardless MV type, size and activity (Fig. 9A). This relationship implies that like venting, also the invisible miniseepage is an expression of the MV activity and it is determined by the same endogenous gas pressure regime. This is consistent with theoretical migration models of seepage related to gas advection processes (Brown, 2000; Etiope et al., 2008). This means that surface mud condition (due to its water content, viscosity and very low permeability) is not the only factor determining the miniseepage flux, but it just modulates, sometimes completely hiding, the subsoil seepage activity. Also, it is evident that miniseepage is often a significant component of the total gas emission of a MV. In type B MVs, where the dry mud area is comparatively much larger than the vent area, miniseepage is generally one order of magnitude (up to two) higher than macro-seep output (e.g. WSD in Taiwan or Regnano, and Nirano in Italy). This relationship can then be applied to those MVs which have only macro-seepage flux measurements, so that the methane budget from these MVs can be more completely assessed.

For the second relationship, area vs. emission factor, it seems that larger MV area usually exhibits smaller emission factor. This may be due to the fact that, generally, larger the MV area, smaller is the ratio between macro-seepage area (area covered by active gas vents) and non-venting mud area. This relationship is further proved by recent study at Chung-Lun (CL) pool in Taiwan (Cheng et al., 2008), a mud pool which emits mostly CO_2 (Yang et al., 2003, 2004). Cheng et al. (2008) measured gas flux from CL pool by using an open funnel and thermal mass flow meter. Their result showed that ~5.5 tons of CH_4 were emitted from this pool that is 300 m^2 large. This fits well with our relationship which provides confidence to our results.

Although CH and LYS are excluded from our calculation, they are still plotted in Fig. 9 for comparison. The poor fitting of these two locations indicates that Eq. (4) is only suitable for MVs and mud pools that continuously emit gas through macro- and miniseepage but not for everlasting fire areas like CH or MVs like LYS that typically emit gas as high pressure "jet" gas venting.

Large uncertainties associated with the two relationships proposed here emphasize the need of more flux data to derive a better model. However, these relationships provide a preliminary but objective way to estimate at least the order of magnitude of the total CH_4 emission from MVs, especially when miniseepage measurements are not possible.

5. Conclusions

This study showed the importance of gas miniseepage as a common and fundamental component of gas emission from mud volcanoes. Data from different mud volcanoes from Taiwan, Italy, Romania and Azerbaijan were examined, leading to the following main conclusions:

(a) About 110 tons of CH_4, 6.3 tons of CO_2, and 0.7 tons of C_2H_6 are estimated to be emitted only by miniseepage from six locations (5 MVs and 1 seep) in SW Taiwan. The miniseepage output represents about ~80% of total emission which includes macro-seepage fluxes (Yang et al. (2004). Periods of increased macro-seepage activity (Chao et al., 2010) may then correspond to higher miniseepage.
(b) Around a dry seep, e.g., CH, methane flux decreases as the distance from the main gas channeling zone increases. This decrease in methane flux is accompanied by an increase of molecular fractionation, so that the methane/ethane ratio is higher for lower seepage. This phenomenon was also observed in other mud volcanoes in Europe and Japan (Etiope et al., 2011).
(c) The subsoil water content and permeability are important factors that may modulate surface miniseepage flux. A good correlation between high electrical resistivity and high gas

flux observed at the WSD MV, suggests that unsaturated subsoil is a preferential zone for shallow gas accumulation and seepage to the atmosphere. This phenomenon also suggests that eventual lack of detectable exhalation in correspondence with wet mud does not mean that gas is up-welling only in correspondence with the craters and vents. Wet mud may just modulate and eventually hide the subsoil seepage activity.

(d) Flux data of 28 MVs from Italy, Romania, Azerbaijan and Taiwan converge to indicate that miniseepage is directly proportional to the vent output and it is a significant component of the total methane budget of a MV: it is generally of the same level of or one order of magnitude higher than the gas output from the vents. Small MVs have a higher emission factor in comparison with large MV due to the smaller ratio between macro-seep area (area covered by active gas vents) and non-venting mud area.

(e) A preliminary miniseepage vs. macro-seep flux equation has been statistically assessed and it can be used to estimate theoretically the flux of miniseepage for MVs of which only the flux from vents is evaluated. The positive correlation between the two parameters suggests that also miniseepage flux, as macro-seepage, is an expression of the MV activity. This will allow a more complete quantification of gas emission in MVs, thus refining also global methane emission estimates.

Acknowledgements

Authors would like to thank T.F. Lan, C.C. Fu, H.F. Lee, C.Y. Wu, C.Y. Cheng, K.W. Wu at the Department of Geosciences in NTU for helping in the collection and analysis of the samples. The authors also would like to thank two anonymous reviewers who provided valuable feedback in refining this article. The National Science Council (NSC97-2116-M-002-021-; 98-2116-M-002-006-/TFY) and Central Geological Survey of Taiwan financially supported this research.

References

Brown, A., 2000. Evaluation of possible gas microseepage mechanisms. American Association of Petroleum Geologists Bulletin 84, 1775–1789.

Cardellini, C., Chiodini, G., Frondini, F., Granieri, D., Lewicki, J., Peruzzi, L., 2003. Accumulation chamber measurements of methane fluxes: application to volcanic-geothermal areas and landfills. Applied Geochemistry 18, 45–54.

Chang, P.Y., Yang, T.F., Chi, L., Hong, W.L., 2010. An observation of the electrical resistivity variation before and after the Pingtung Earthquake in the Wushanting Mud Volcano Area in Southwestern Taiwan. Journal of Environmental and Engineering Geophysics 15, 213–219.

Chao, H.-C., You, C.-F., Sun, C.-H., 2010. Gases in Taiwan mud volcanoes: chemical composition, methane carbon isotopes, and gas fluxes. Applied Geochemistry 25, 428–436.

Cheng, C.Y., Heinicke, J., Fu, C.C., Yang, T.F., Tong, L.T., 2008. Emission flux of CO_2 through an active fault zone in SW Taiwan. Eos Transactions American Geophysical Union, 89(53), Fall Meeting Supplementary, Abstract U41B-0015.

Chiu, J.K., Tseng, W.H., Liu, C.S., 2006. Distribution of gassy sediments and mud volcanoes offshore southwestern Taiwan. Terrestrial Atmospheric and Oceanic Sciences 17, 703–722.

Chuang, P.C., Yang, T.F., Lin, S., Lee, H.F., Lan, T.F.F., Hong, W.L., Liu, C.S., Chen, J.C., Wang, Y., 2006. Extremely high methane concentration in bottom water and cored sediments from offshore southwestern Taiwan. Terrestrial Atmospheric and Oceanic Sciences 17, 903–920.

Chuang, P.C., Yang, T.F., Hong, W.L., Lin, S., Sun, C.H., Lin, A.T.S., Chen, J.C., Wang, Y., Chung, S.H., 2010. Estimation of methane flux offshore SW Taiwan and the influence of tectonics on gas hydrate accumulation. Geofluids 10, 497–510.

Cramer, S.D., 1984. Solubility of methane in brines from 0 to 300 C. Industrial and Engineering Chemistry Process Design and Development 23 (3), 533–538.

Dimitrov, L.I., 2002. Mud volcanoes – the most important pathway for degassing deeply buried sediments. Earth-Science Reviews 59, 49–76.

EMEP/EEA, 2009. EMEP/EEA air pollutant emission inventory guidebook – 2009. Technical guidance to prepare national emission inventories. European Environment Agency Technical Report No 6/2009. European Environment Agency, Copenhagen. doi: http://dx.doi.org/10.2800/23924.

Etiope, G., Klusman, R., 2010. Microseepage in drylands: flux and implications in the global atmospheric source/sink budget of methane. Global and Planetary Change 72, 265–274.

Etiope, G., Milkov, A.V., 2004. A new estimate of global methane flux from onshore and shallow submarine mud volcanoes to the atmosphere. Environmental Geology 46, 997–1002.

Etiope, G., Caracausi, A., Favara, R., Italiano, F., Baciu, C., 2002. Methane emission from the mud volcanoes of Sicily (Italy). Geophysical Research Letters 29 (8), 1215. http://dx.doi.org/10.1029/2001GL014340.

Etiope, G., Baciu, C., Caracausi, A., Italiano, F., Cosma, C., 2004a. Gas flux to the atmosphere from mud volcanoes in eastern Romania. Terra Nova 16, 179–184.

Etiope, G., Feyzullayev, A., Baciu, C.L., Milkov, A.V., 2004b. Methane emission from mud volcanoes in eastern Azerbaijan. Geology 32, 465–468.

Etiope, G., Guerra, M., Raschi, A., 2005. Carbon Dioxide and Radon Geohazards over a Gas-bearing Fault in the Siena Graben (Central Italy). Terrestrial, Atmospheric and Oceanic Sciences 16, 885–896.

Etiope, G., Martinelli, G., Caracausi, A., Italiano, F., 2007. Methane seeps and mud volcanoes in Italy: gas origin, fractionation and emission to the atmosphere. Geophysical Research Letters 34, L14303.

Etiope, G., Milkov, A.V., Derbyshire, E., 2008. Did geologic emissions of methane play any role in quaternary climate change? Global and Planetary Change 61, 79–88.

Etiope, G., Feyzullayev, A., Baciu, C.L., 2009. Terrestrial methane seeps and mud volcanoes: a global perspective of gas origin. Marine Petroleum Geology 26, 333–344.

Etiope, G., Nakada, R., Tanaka, K., Yoshida, N., 2011. Gas seepage from Tokamachi mud volcanoes, onshore Niigata Basin (Japan): origin, post-genetic alterations and CH_4-CO_2 fluxes. Applied Geochemistry 26 (3), 348–359.

Guliyev, I., Feizullayev, A., 1997. All about Mud Volcanoes. Geology Institute, Azerbaijan Academy of Sciences.

Hernandez, P., Perez, N., Salazar, J., Nakai, S., Notsu, K., Wakita, H., 1998. Diffuse emission of carbon dioxide, methane, and helium-3 from Teide volcano, Tenerife, Canary Islands. Geophysical Research Letters, 25.

Howell, D., 2002. Statistical Methods for Psychology. Duxbury Press, Belmont, CA.

Huang, C.Y., Wu, W.Y., Chang, C.P., Tsao, S., Yuan, P.B., Lin, C.W., Xia, K.Y., 1997. Tectonic evolution of accretionary prism in the arc-continent collision terrane of Taiwan. Tectonophysics 281, 31–51.

Huang, C.Y., Yuan, P.B., Tsao, S.J., 2006. Temporal and spatial records of active arc-continent collision in Taiwan: a synthesis. Geological Society of America Bulletin 118, 274–288.

Klusman, R., Leopold, M., LeRoy, M., 2000. Seasonal variation in methane fluxes from sedimentary basins to the atmosphere: results from chamber measurements and modeling of transport from deep sources. Journal of Geophysical Research-Atmospheres 105 (D20), 24661–24670.

Lan, T.F., Yang, T.F., Lee, H.F., Chen, Y.G., Chen, C.H., Song, S.R., Tsao, S., 2007. Compositions and flux of soil gas in Liu-Huang-Ku hydrothermal area, northern Taiwan. Journal of Volcanology and Geothermal Research 165, 32–45.

Lee, H.F., Yang, T.F., Lan, T.F., Song, S.R., Tsao, S., 2005. Fumarolic gas composition of the Tatun Volcano Group, northern Taiwan. Terrestrial Atmospheric and Oceanic Sciences 16, 843–864.

Lin, S., Hsieh, W.C., Lim, Y.C., Yang, T.F., Liu, C.S., Wang, Y., 2006. Methane migration and its influence on sulfate reduction in the Good Weather Ridge region, South China Sea continental margin sediments. Terrestrial Atmospheric and Oceanic Sciences 17, 883–902.

Lin, A.T., Liu, C.S., Lin, C.C., Schnurle, P., Chen, G.Y., Liao, W.Z., Teng, L.S., Chuang, H.J., Wu, M.S., 2008. Tectonic features associated with the overriding of an accretionary wedge on top of a rifted continental margin: an example from Taiwan. Marine Geology 255, 186–203.

Livingston, G., Hutchinson, G., 1995. Enclosure-based measurement of trace gas exchange: applications and sources of error. In: Matson, P., Harriss, R. (Eds.), Biogenic Trace Gases: Measuring Emissions from Soil and Water. Blackwell Scientific Publications, London, pp. 14–51.

Milkov, A.V., 2000. Worldwide distribution of submarine mud volcanoes and associated gas hydrates. Marine Geology 167, 29–42.

Mouthereau, F., Lacombe, O., Deffontaines, B., Angelier, J., Brusset, S., 2001. Deformation history of the southwestern Taiwan foreland thrust belt: insights from tectono-sedimentary analyses and balanced cross-sections. Tectonophysics 333, 293–318.

Norman, J.M., Kucharik, C.J., Gower, S.T., Baldocchi, D.D., Crill, P.M., Rayment, M., Savage, K., Striegl, R.G., 1997. A comparison of six methods for measuring soil-surface carbon dioxide fluxes. Journal of Geophysical Research-Atmospheres 102, 28771–28777.

Spulber, L., Etiope, G., Baciu, C., Maloss, C., Vlad, S.N., 2010. Methane emission from natural gas seeps and mud volcanoes in Transylvania (Romania). Geofluids 10 (4), 463–475.

Thielemann, T., Lucke, A., Schleser, G.H., Littke, R., 2000. Methane exchange between coal-bearing basins and the: the Ruhr Basin and the Lower Rhine Embayment, Germany. Organic Geochemistry 31, 1387–1408.

Wilks, D., 2006. Statistical Methods in the Atmospheric Sciences. Academic Press.

Yang, T.F., Chou, C.Y., Chen, C-H., Chyi, L.L., Jiang, J.H., 2003. Exhalation of radon and its carrier gases in SW Taiwan. Radiation Measurements 36, 425–429.

Yang, T.F., Yeh, G.H., Fu, C.C., Wang, C.C., Lan, T.F., Lee, H.F., Chen, C.H., Walia, V., Sung, Q.C., 2004. Composition and exhalation flux of gases from mud volcanoes in Taiwan. Environmental Geology 46, 1003–1011.

Yang, T.F., Chuang, P.C., Lin, S., Chen, J.C., Wang, Y., Chung, S.H., 2006. Methane venting in gas hydrate potential area offshore of SW Taiwan: evidence of gas analysis of water column samples. Terrestrial Atmospheric and Oceanic Sciences 17, 933–950.